Servo-Position Control with Dynamic Lag Precompensator for Pmsm Drives

Vittek Ján, Makyš Pavol, Štulrajter Marek
University of Žilina, Faculty of Electrical Engineering, SK

Dodds, Stephen J., Perryman, Roy
University of East London, School of Computing Engineering, UK

***Abstract* - The paper presents design of *near-time-optimal* position control of electrical drive with permanent magnet synchronous motor. The principles of time-optimal-control and forced dynamic control are combined to form a novel method of achieving a nearly time optimal position control performance in drives equipped with controllers enabling close following of time varying reference position inputs from 'near time optimal' model. For compensation of the dynamic lag between model generated position and the real drive position response a precompensator is implemented. The simulations and experimental results show possibility to achieve '*near time optimal*' behavior of the drive.**

***Index Terms* - Vector control, Feedback linearisation, Time optimal control, Permanent magnet synchronous motor.**

I. INTRODUCTION

In many applications of position controlled electrical drives it is desirable to achieve the demanded position in the minimum possible time within the limitations imposed by available hardware. This can be achieved by means of the 'time optimal control', which is a form of 'bang-bang' control in which control variable switches between its saturation limits. Such control system then suffers from limit cycling with no damping upon approaching the reference position. To solve this problem some modifications of the 'time optimal control' were introduced. Small price to pay for the limit cycle elimination measures and the assumption of zero friction is that the settling time is increased slightly with respect to the theoretical one and therefore the phrase 'near time optimal' is introduced.

For the development of suitable control system for changing the position of one degree of freedom the principles of forced dynamic control [1], [2] and time optimal control [3], [4] are combined to form 'near time optimal' control algorithm. The dynamic behaviour of the drive is further improved by adding of precompensator into control system.

Forced dynamic control, based on the principles of vector control [5], [6] and feedback linearisation [7], [8], is a relatively new method for control of AC drives. In the permanent magnet synchronous motor (PMSM) application, mutual orthogonality of the torque producing stator current vector and rotor magnetic flux vector is maintained as in conventional vector control. The control system has a shaft sensorless inner speed control loop utilising a speed estimation algorithm based on current and voltage measurements. This loop has linear first order dynamics with an adjustable time constant.

The reason for utilising this control method of ac drives is that it is relatively easy to design the control system to closely follow a time varying position reference input with predictable tracking errors [9], [10]. An outer position control loop with an adjustable gain is then closed via a suitable position measurement. The system automatically counteracts load torque by producing a nearly equal and opposite control torque component, provided by a load torque observer.

The system is made almost time optimal by the novel use of a software-implemented model of a closed-loop time optimal control system of the mechanism, utilising a non-linear switching boundary in the state space which adapts to the load torque estimate from the load torque observer. Control chatter is eliminated from the model by introduction of a boundary layer and a linear term to the switching boundary equation. The position output from this model forms the reference input to the outer position control loop, which responds with a relatively small position error. It is important to note that the drive position controller does not have to be '*near time optimal*'. For further improvement of the dynamical

response the dynamic lag precompensator was added. Precompensator eliminates the dynamic lag between the continuously varying model output and the actual rotor position so that the motion of the real mechanism is 'near time optimal' through being slaved precisely to that of the model. The experiment results presented show good agreement with theoretical predictions.

II. NEAR-TIME-OPTIMAL CONTROL

2.1. *Control System Structure*

Time optimal control theory was introduced via 'Maximum Principle' of L. S. Potryagin, the most important result of which is that the control function of an n^{th} order plant subject to the control saturation constraints, $|u| \le u_{max}$, is a '*bang-bang*' control function switching between the extreme values, $\pm u_{max}$ and having a finite number of $n-1$ switches, where n is the order of the plant [3]. The mathematical expression for the time-optimal switching boundary in the state space needed for closed-loop implementation is rather complicated for plants of greater than second order.

However switching boundaries yielding time optimal control for first or second order plants are easily obtained and applicable to many electrical drive applications. Therefore a reduced second order model is used here to derive a closed-loop time optimal controller. The drawback with this approach, however, is that any un-modelled dynamic lags in the system might give rise to unacceptable overshooting in the transient response and limit cycling behavior about a constant set-point. The proposed exploitation of a real time model of the reduced order time optimal control system circumvents this problem. The behavior of the closed-loop time optimal control model can be made free of any overshooting or limit cycling because the plant of this model is well known. The position response of this model then provides the reference input for the drive control loop. The stability of the closed-loop system, which structure is shown in Fig.1, then depends entirely on the drive control loop.

It is assumed that rotor angle demand, $\vartheta_m(t)$, is piecewise constant. The time optimal switching boundary is dependent on the load torque and hence its estimate is fed back to the closed-loop time-optimal-control model. The fact that the drive control loop is not based on a time optimal control law will not prevent the overall system from approaching closely to time-optimality. All that is required is for the drive control loop to make the rotor angle, $\vartheta_r(t)$ follow $\vartheta_m(t)$ with a small error such that $|\vartheta_m(t) - \vartheta_r(t)| << |\Delta\vartheta_d|$, where $\Delta\vartheta_d$ is the *change* of ϑ_d. If, however, too large a value of $\Delta\vartheta_d$ was applied, the motor would be forced into its torque saturation limits and the actual settling time would not only be longer than T_s, but also longer than T_{opt} due to the sub-time-optimality of the drive control loop.

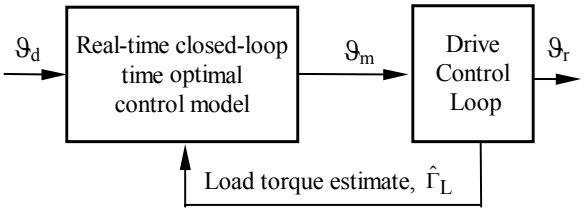

Fig. 1. Basic control system structure

In the system of Fig. 1, a step input is *never* applied to the drive control loop. Instead, $\vartheta_m(t)$ is continuously varying and is very close to the true time optimal response of the drive. In making $\vartheta_r(t)$ follow $\vartheta_m(t)$, the drive control loop *automatically* causes the motor torque at first to swing between values approaching the maximum limits to achieve near-time-optimal control.

2.2. *Closed-Loop Time-Optimal-Control Model*

Fig. 2 shows a block diagram of the double integrator plant model upon which the closed-loop time optimal control model is developed.

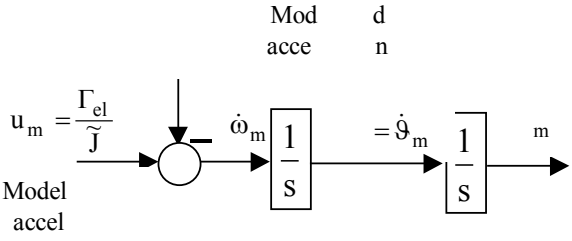

Fig. 2. Double integrator model as a base for near time optimal control

The model control law is developed by considering the phase-portrait for $u_m = \pm u_{max}$, where, u_{max} is the maximum available control acceleration from the electrical drive. In this case, the plant state differential equations are:

$$\dot{\vartheta}_m = \omega_m$$

$$\dot{\omega}_m = \frac{1}{\tilde{J}_r}\left(\Gamma_{el} - \hat{\Gamma}_L\right), \ |\Gamma_{el}| \le \Gamma_{max} \qquad (1a,b)$$

The general state trajectory is the solution of the *state trajectory differential equation* obtained by dividing (1b) by (1a):

$$\frac{\dot{\omega}_m}{\dot{\vartheta}_m} = \frac{\Gamma_{el} - \hat{\Gamma}_L}{J\dot{\vartheta}_m} \qquad (2)$$

For constant electrical torque and constant load torque equation (2) can be solved analytically yielding the trajectory equation.

$$\vartheta_m(t) = \vartheta_m(0) + \frac{\tilde{J}}{2\left(\Gamma_{el} - \tilde{\Gamma}_L\right)}\left[\omega_m^2 - \omega_m^2(0)\right] \qquad (3)$$

In this initial investigation, the load torque, $\hat{\Gamma}_L$, is assumed constant and the demanded rotor angle, ϑ_d, is constant. The time optimal control of such a plant has one switch during the period of the state trajectory leading to the desired state.

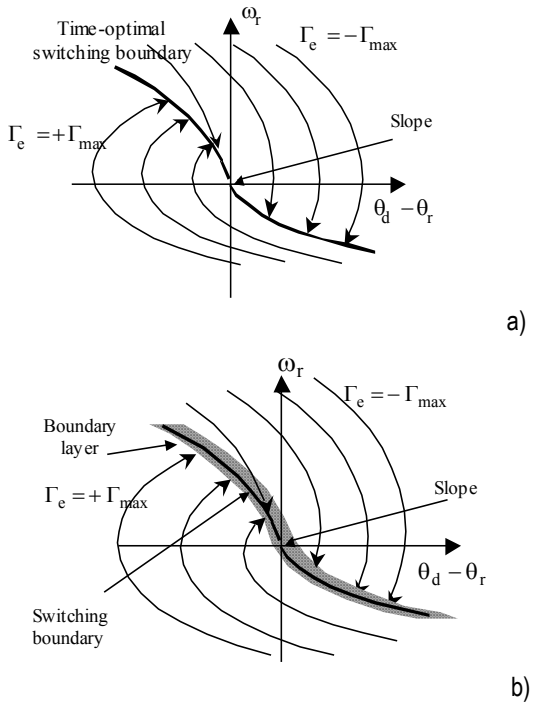

Fig. 3. Switching boundary and close-loop phase portrait

In this case, the time optimal switching boundary comprises two parabolic segments coincident with the two trajectories leading directly to the origin of the error phase plane for $\Gamma_{el} = +\Gamma_{max}$ and $\Gamma_{el} = -\Gamma_{max}$. These are sketched as a function of position errer in Fig. 3a for $\hat{\Gamma}_L > 0$, together with the closed-loop phase portrait in Fig. 3b.

For digital implementation, control chatter and oscillations about the phase-plane origin are eliminated by replacement of the switching boundary by a boundary layer and introduction of a linear velocity feedback term into the model control law, which is as follows:

$$\Gamma_{el} = -\Gamma_{max}\,\mathrm{sat}\left\{\frac{\vartheta_m - \vartheta_d - T_c\omega_m}{-\frac{\tilde{J}_r}{2}\frac{\omega_m^2}{\Gamma_{max}^2 - \hat{\Gamma}_L^2}\left[\hat{\Gamma}_L - \Gamma_{max}\,\mathrm{sign}(\omega_m)\right]}, \ K\right\} \qquad (4)$$

where $\mathrm{sat}(e, K) = \begin{cases} Ke \ \text{for} \ K|e| < 1 \\ \mathrm{sign}(e) \ \text{for} \ K|e| \ge 1 \end{cases}$. Equation (4) is used to create output of the real time closed loop near-time-optimal control model.

Another important feature of the system is the representation of the motor and its mechanical load as it is shown in Fig. 4.

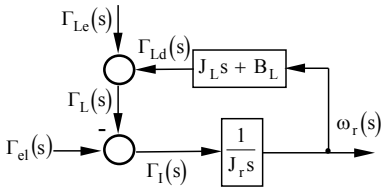

Fig. 4. Representation of motor and its load

Thus only the motor rotor inertia is included in the forward path as a rigid body moving *without friction*. The dynamics of the driven mechanism (including any significant bearing friction), is represented by its inverse dynamics in the feedback path, producing a dynamic component, Γ_{Ld}, of the load torque, Γ_L, as shown. The external load torque component, Γ_{Le}, is added in the usual way. It is also important to note that it is unnecessary to provide an accurate model of the inverse load dynamics in Fig. 2. It is sufficient to obtain an accurate estimate, $\hat{\Gamma}_L$, of the load torque and this may be obtained from a suitable observer [2], [11].

2.3. *Drive Control Loop*

The motor model on which the drive control loop designs are based are as follows. First, the synchronous motor model is formulated in the (d,q) co-ordinate system rotating at synchronous speed:

$$\frac{d}{dt}\begin{bmatrix} i_d \\ i_q \end{bmatrix} = \begin{bmatrix} \frac{-R_S}{L_d} & -p\omega_r \frac{L_q}{L_d} \\ p\omega_r \frac{L_d}{L_q} & \frac{-R_S}{L_q} \end{bmatrix} \begin{bmatrix} i_d \\ i_q \end{bmatrix} - \frac{p\omega_r}{L_q}\begin{bmatrix} 0 \\ \Psi_{PM} \end{bmatrix} + \begin{bmatrix} \frac{1}{L_d} & 0 \\ 0 & \frac{1}{L_q} \end{bmatrix} \begin{bmatrix} u_d \\ u_q \end{bmatrix}$$

$$\frac{d\omega_r}{dt} = \frac{1}{J_r}\left\{c\cdot\left[\Psi_{PM} i_q + \left(L_d - L_q\right) i_d\, i_q\right] - \Gamma_L\right\} = \frac{1}{J_r}\left\{\Gamma_{el} - \Gamma_L\right\}$$

$$\frac{d\vartheta_r}{dt} = \omega_r \qquad (5a,b,c)$$

Here $I^T = \begin{bmatrix} i_d & i_q \end{bmatrix}$ and $U^T = \begin{bmatrix} u_d & u_q \end{bmatrix}$ are, respectively, column vectors whose elements are the stator current and voltage components *(this notation being convenient for development of the control algorithm*), ω_r and ϑ_r are the rotor velocity and position, p is number of pole-pairs, c is constant c=3p/2, Γ_L is the external load torque, R_S is the phase resistance, L_d and L_q are the direct and quadrature phase inductances, Ψ_{PM} is permanent magnetic flux and J_r is the lumped moment of inertia.

The control strategy for the synchronous motor is based on *feedback linearisation* [5], forming a non-linear multivariable control law to obtain a prescribed linear speed dynamics together with the vector control condition of mutual orthogonality between the stator current and rotor flux vectors (*assuming perfect estimates of the plant parameters*). Estimates of the rotor speed and the load torque, required by the control algorithm, are obtained from two special observers [1], [2]. The drive is rendered robust with respect to the external load torque and changes in the dynamics of the driven mechanical load by incorporating load torque compensation in the control algorithm. An important feature of this system is that *the rotor speed is controlled* with a *closed-loop time constant chosen by the control system designer*. The rotor angular velocity is made to satisfy:

$$\frac{d\omega_r}{dt} = \frac{1}{T_\omega}\left(\omega_d - \omega_r\right) \qquad (6)$$

The technique is to equate the right hand side of this equation with the right hand side of the corresponding motor equation (5b). The result is the rotor speed *linearising* equation. This forces the non-linear differential equation (5b) to have the same response as the linear equation (6). The linearising equation is as follows:

$$\frac{1}{J}\left\{c_5\left[\psi_d i_q - \psi_q i_d\right] - \Gamma_L\right\} = \frac{1}{T_\omega}\left(\omega_d - \omega_r\right) \qquad (7)$$

where $\psi_d = L_d i_d + \Psi_{PM}$ and $\psi_q = L_q i_q$ are the magnetic flux components.

The second part of the control law is formulated on the basis of vector control which, in geometric terms, requires that the rotor magnetic flux vector is at the right angles to the stator current vector. For surface mounted magnets of synchronous motor up to nominal speed is maximal torque achieved, [6] for:

$$i_d = 0 \qquad (8)$$

By solving equations (7) and (8) the following expressions for the demanded values of the current components are obtained:

$$i_{d\_d} = 0$$
$$i_{q\_d} = \frac{1}{\tilde{c}_5 \Psi_{PM}}\left[\hat{\Gamma}_L + \frac{\tilde{J}_r}{T_\omega}\left(\omega_d - \hat{\omega}_r\right)\right] \qquad (9)$$

where estimates of $\hat{\omega}_r$ and $\hat{\Gamma}_L$ are obtained from the suitable observer algorithms [11], [12]. The stator current demands are realised by the usual current loops realised by the switched power electronic circuits. Control law equation (9) yields a rotor speed response with linear, first order dynamics and unity dc gain, the closed-loop time constant, T_ω, being chosen by the system designer. Thus:

$$\frac{\omega_r(s)}{\omega_d(s)} = \frac{1}{1 + sT_\omega} \qquad (10)$$

2.4. *Position Feedback and Precompensator*

It remains to close a position loop around this speed control system. It is done in two steps.

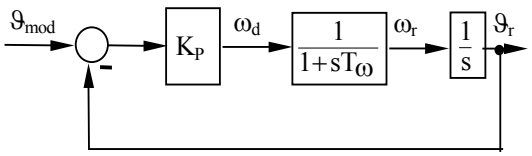

Fig. 5. Block diagram of drive control loop

First, as it is shown in the block diagram of Fig. 5 only proportional gain multiplies the error between model and real position.

It is straightforward to show that the parameters, K_P and T_ω can be adjusted to yield any desired second order closed-loop transfer function. For example a settling time, T_s, to 95% of the step response, can be realized by coincident closed loop poles at $s = -9/2T_s$, the closed-loop transfer function being:

$$\frac{\vartheta_{mod}(s)}{\vartheta_r(s)} = \left(\frac{1}{1 + 2s\,T_s/9}\right)^2 \tag{11a}$$

$$K_P = 9/4T_s \quad \text{and} \quad T_\omega = T_s/9 . \tag{11b}$$

The second approach with precompensator is shown in the block diagram of Fig. 6. For its design it is necessary to know the closed loop dynamic of the electrical drive position controller, which is shown in Fig. 5 and done by equations (11a).

The next step is to create precompensator, which is the inverse of the closed/loop transfer function (11a):

$$F_{PC}(s) = \frac{\vartheta_{mod}(s)}{\vartheta_m(s)} = s^2\,\frac{4T_s^2}{81} + s\,\frac{4T_s}{9} + 1 \tag{12}$$

Figure 6 shows block diagram with transfer functions of the position controlled system and precompensator and Fig. 7 shows complete implementation of precompensator.

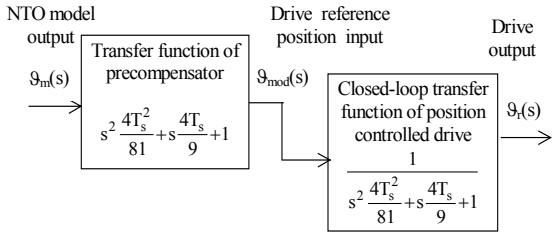

Fig. 6. Precompensator for zero dynamic lag

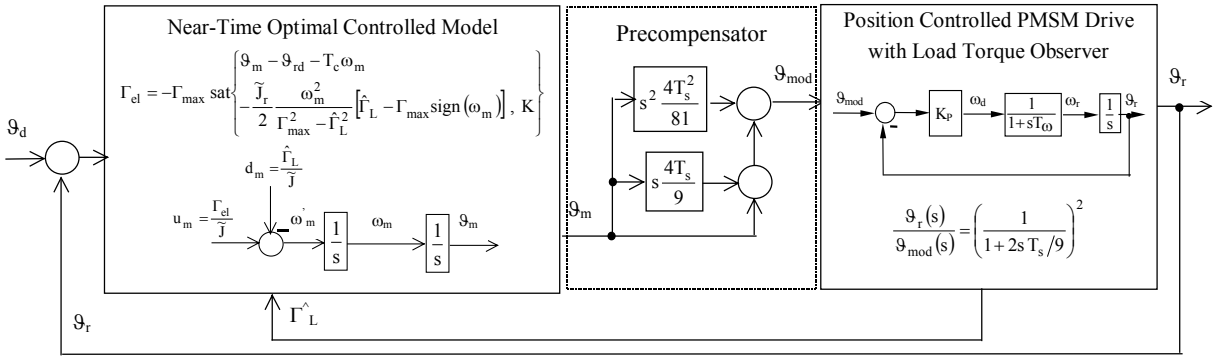

Fig. 7. Complete '*near-time optimal*' position control system with dynamic lag precompensation

2.5. *Load Torque Observer*

The real time model of the load torque observer is based on the differential equations for the motor position and speed, (5b) and (5c) together with the differential equation for the load torque . The load torque is treated as a state variable, which is assumed to be constant, therefore its differential equation is simply, $\dot{\hat{\Gamma}}_L = 0$. The observer equations correspondto those of the real plant, when the error between observer's input and output, $e_\vartheta = \vartheta_r - \hat{\vartheta}_r$ multiplied with corresponding gains is added into every observer correction loop (13):

$$\begin{aligned}
\dot{\hat{\vartheta}}_r &= \hat{\omega}_r + k_\vartheta e_\vartheta \\
\dot{\hat{\omega}}_r &= \frac{1}{J}\left[c_5\left(\Psi_q i_d - \Psi_d i_q\right) - \hat{\Gamma}_L\right] + k_\omega e_\vartheta \\
\dot{\hat{\Gamma}}_L &= 0 + k_\Gamma e_\vartheta
\end{aligned} \tag{13}$$

where $\hat{\vartheta}_r$, $\hat{\omega}_r$ and $\hat{\Gamma}_L$ are, respectively estimates of ϑ_r, ω_r and Γ_L. The observer correction loop is actuated using the error between the measured rotor position and its estimate from the observer as can be seen from Fig. 3a. Equations (13) are then numerically integrated by the Euler explicit formula using the iteration interval corresponding to the achieved sampling frequency.

Equations (13) constitute a conventional third order linear observer [13] with a correction loop characteristic polynomial, which may be chosen via the gains k_θ, k_ω and k_Γ. If all three observer poles are placed at $s=-\omega_0$, then the filtering time constant, T_f, corresponding to (11b) satisfies $\omega_0=6/T_f$ (*for n=3*) and is a single design parameter. Comparing the observer characteristic polynomial with the prescribed one the gains can be calculated as follows:

$$s^3+\frac{18}{T_f}s^2+\frac{108}{T_f^2}s+\frac{216}{T_f^3}=s^3+k_\vartheta s^2+k_\omega s+\frac{k_\Gamma}{J} \qquad (14a)$$

$$k_\Gamma=\frac{216J}{T_f^3};\ k_\omega=\frac{108}{T_f^2};\ k_\vartheta=\frac{18}{T_f};\ \text{for } T_f=\frac{6}{\omega_0} \qquad (14b)$$

For the selection of ω_0 a rule of thumb which is $\omega_0<5/h_0$ may be taken such, that the discrete time correction loop behavior approximates to that of the theoretical continuous observer (h_0 - *sampling period*).

Although the load torque is assumed constant in the formulation of its real time model the estimate, $\hat{\Gamma}_L$, will follow an arbitrarily time varying disturbance torque and will do it more closely as T_f is reduced, but at the expense of sensitivity to any noise in rotor position measurement. If the rotor speed is measured, then the alternative observer for load torque estimation shown in the block diagram of Fig. 3b can be employed.

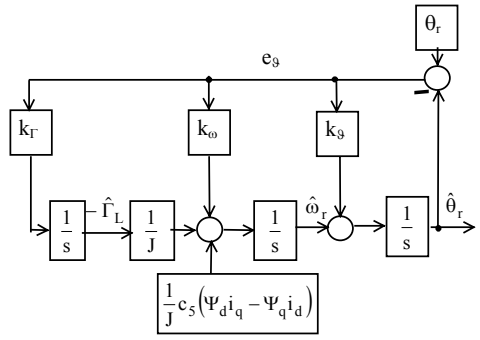

Fig. 8: Load torque observer from rotor position measurement.

III. Simulation And Experimental Results

The simulations and preliminary experiments were performed with iddle running a DutymAx DS PMSM having the following parameters:- P_n=375 W at ω_n=314,16 rad/s; p=3; R_s=36,5 Ω; $L_d=L_q$=50 mH; Ψ_{PM}=0,312 Vs; J_r=0,032 kgm^2. A sampling frequency of 10 kHz was achieved during implementation. The control algorithms were implemented on a Pentium PC. The stator currents were measured through LEM transformers and evaluated using a PC Lab Card PL818 built into the PC. A six-transistor IGBT module was used as the three-phase inverter. All the experiments presented were carried out with a DC supply voltage of U_{dc}=200 V.

The simulation results are shown in Fig. 9a and Fig 9b for control system, which corresponds to control system without and with precompensator. The demanded position for both cases was φ_{dem} =50 rad.

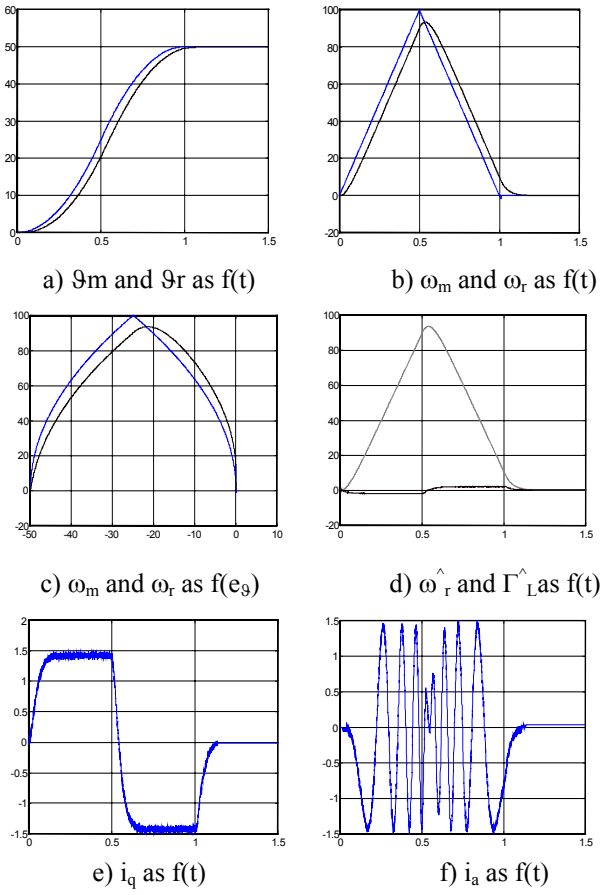

Fig. 9.a: Simulation results for outer loop with proportional gain.

The graphical results comprise:

(a) position of the near time optimal model and real rotor position as a function of time,

(b) speed of the model and real rotor speed as a function of time,

(c) position of the model and rotor position as a function of model and rotor speed,

(d) estimated rotor speed (*not used in the control algorithm*) and load torque (*multiplied by 10*) from the filtering observer,

(e) i_q stator current component as a function of time and phase 'a' current as a function of time.

Fig. 10 shows corresponding experimental results for the near-time-optimal position control system and idle running PMSM without precompensator. Due to technical problems the precompensator was not implemented yet.

The variables of the near-time-optimal controlled model are displayed as blue coloured graphs to distinguish them from the drive responses (black).

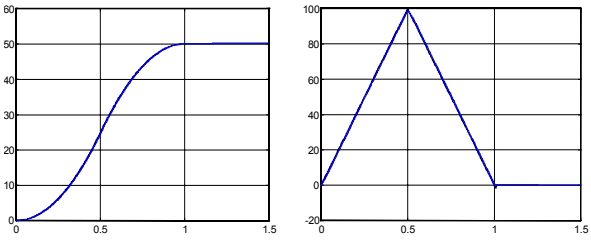

a) ϑm and ϑr as f(t) b) ω_m and ω_r as f(t)

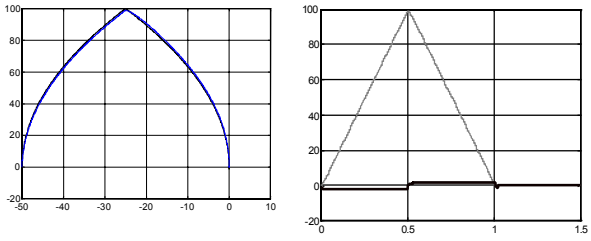

c) ω_m and ω_r as f(e_ϑ) d) $\hat{\omega}_r$ and $\hat{\Gamma}_L$ as f(t)

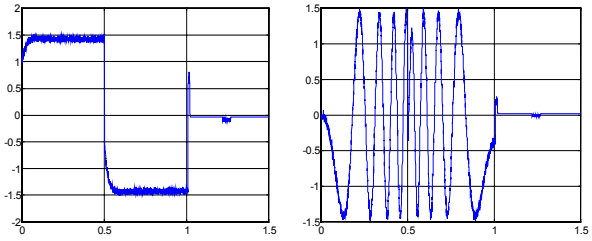

e) i_q as f(t) f) i_a as f(t)

Fig. 9.b: Simulation results for control loop with precompensator.

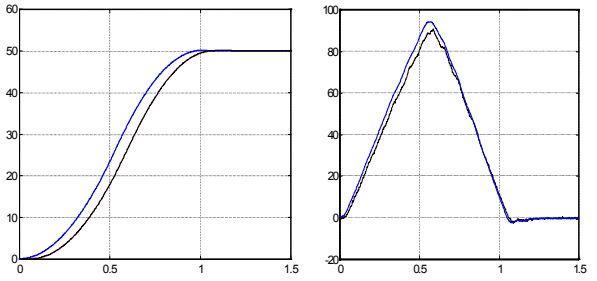

a) ϑ_m and ϑ_r as f(t) b) ω_m and ω_r as f(t)

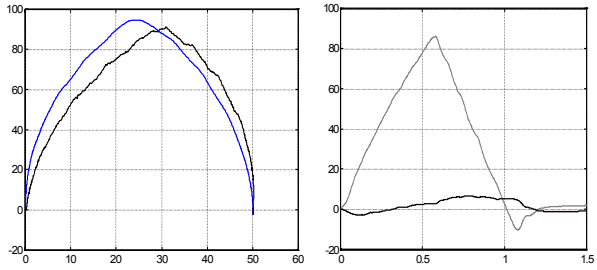

c) ω_m and ω_r as f(e_ϑ) d) $\hat{\omega}_r$ and $\hat{\Gamma}_L$ as f(t)

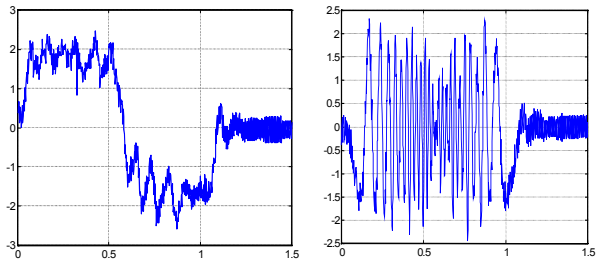

e) i_q as f(t) f) i_a as f(t)

Fig. 10: Experimental results for '*near-time optimal control*' without precompensator.

IV. Conclusions And Recommendations

The simulation and preliminary experimental results presented for no load state show the possibility of forcing a drive, via a time-optimal model to respond nearly time optimally to responses to step changes in the demanded position.

As it was shown in simulations the accuracy with which this is this achieved could be improved through implementation of precompensator. Therefore the implementation of the precompensator in experiments is the most important suggestion for future research work.

Also further investigations of load torque estimation are recommended for loaded drive. The tracking accuracy for small, slowly varying reference positions should also be investigated.

ACKNOWLEDGEMENT

The authors wish to thank to the 'Deutscher Akademischer Austauschdienst' for funding the bilateral research project No. 04/2003 "*R&D of a Sensorless μP-Controlled AC Drives Employing Synchronous Rotating and Linear Motors*" together with 'Czech and Slovak Joined Commission' for funding the bilateral research project No.016/023, "*Analysis and Development of a Modern Controlled Electric Drives"*.

REFERENCES

[1] S. J. Dodds, J. Vittek and R. Perryman, "Forced Dynamic Control of Shaft Sensorless Induction Motor Drives," *Proceedings of Speedam'98 conference*, Sorrento, Italy, 1998, pp. A1-9 – A1-14.

[2] S. J. Dodds, J. Vittek, R. Perryman, R. and J. Altus, "Preliminary Experimental Results for Synchronous Motor Drives with Forced Dynamics," *Proceedings of IASTED CA'98 conference*, Honolulu, USA, 1998, pp.219 – 223.

[3] E. P. Ryan, "*Optimal Relay and Saturating Control System Synthesis*," Peter Pregrinus, 1982.

[4] W. Leonhard, "*Control of Electrical Drives*," Springer-Verlag, 1997.

[5] I. Boldea, A. S. Nasar, "*Vector Control of AC Drives*," 2nd edition, CRC Press, 1992.

[6] D. W. Nowotny, T. A. Lipo, "*Vector Control and Dynamics of AC Drives*," Clarendon Press 1969.

[7] A. Isidori, "*Nonlinear Control Systems*," 2nd edition, Springer-Verlag, 1989.

[8] M. Krstic, I. Kanellakopoulos, P. Kokotovic, "*Nonlinear and Adaptive Control Design,*" John Wiley and Sons, 1995.

[9] J. Vittek, T. Baculak, S. J. Dodds, and R. Perryman, "Near-Time-Ooptimal Position Control of Electrical Drives with Permanent Magnet Synchronous Motor," *Proceedings of EPE 2003 conference*, Toulouse, France, 2003, CD Rom.

[10] S. Brock, J. Deskur and K. Zawirski, "A Modified Approach to the Design of Robust Speed and Position Control of Servo-Drives," *Proceedings of EPE'PEMC 2002 conference*, Cavtat, Croatia, 2002, CD Rom.

[11] D. Hamada, K. Uchida, F. Yusivar, H. Haratsu, S. Wakao and T. Onuki, "Sensorless Control of PMSM using Linear Reduced Order Observer including Disturbance Torque Estimation," *Proceedings of EPE'99 conference,* Lausanne, Switzerland, 1999, pp. 312-317.

[12] V. Comnac, M. Cernat, F. Moldoveanu and R. Ungar, "Variable Structure Control of Surface Permanent Magnet Synchronous Machine (SPMSM)," *Proceedings of PCIM'99 conference*, Nuremberg, Germany, 1999, pp. 351 – 356.

[13] N. S. Nise, "*Control System Engineering,*" The Benjamin Cumming Publishing Company, Inc., Redwood City, Ca, 1995.

[14] P. Korondi, D. K. Young and H. Hashimoto, "Sliding Mode Based Disturbance Compensation for Motion Control," *Proceedings of IEEE IECON'97 conference*, New Orleans, USA, 1997, pp.73-78.

[15] O. Aguilar, A. G. Loukianov and J. M. Canedo, "Observer-based Sliding Mode Control of Synchronous Motor," *Proceedings of IFAC'2002 congress* on *'Automatic Control*', dec. 2002, Guadalajara, Mexico, CD Rom.